

Deterministic and stochastic ensemble KF approaches for 1D Korteweg de Vries (KdV) PDE

Harsha Vaddireddy

School of Mechanical & Aerospace Engineering,
Oklahoma State University,
`hvaddir@okstate.edu`

June 26, 2020

1 Introduction

Korteweg and de Vries derived the KdV equation to model Russell's phenomenon of solitons [1,5]. The KdV equation also appears when modelling the behavior of magneto-hydrodynamic waves in warm plasma's, acoustic waves in an inharmonic crystal and ion-acoustic waves [3]. Many different forms of the KdV equation available in the literature but we use the form,

$$u_t = 6uu_x - u_{3x}, \quad (1)$$

where $u(x, t)$ is generally velocity field with $x \in [-8, 8]$ and $t \in [0, 1.0]$. The term uu_x describes the sharpening of the wave and u_{3x} the dispersion (i.e., waves with different wave lengths propagate with different velocities). The balance between these two terms allows for a propagating wave with unchanged form. The primary application of solitons today are in optical fibers, where the linear dispersion of the fiber provides smoothing of the wave, and the non-linear properties give the sharpening. The result is a very stable and long-lasting pulse that is free from dispersion, which is a problem with traditional optical communication techniques.

2 Numerical Simulation

As the KdV PDE is a stiff nonlinear system, we chose higher order central spatial discretization for first and third order terms in Eq.5

$$\left. \begin{aligned} u_x &= \frac{u_{i+3}^n - 9u_{i+2}^n + 45u_{i+1}^n - 45u_{i-1}^n + 9u_{i-2}^n - u_{i-3}^n}{60dx} \\ u_{3x} &= \frac{7u_{i+4}^n - 72u_{i+3}^n + 388u_{i+2}^n - 488u_{i+1}^n + 488u_{i-1}^n - 388u_{i-2}^n + 72u_{i-3}^n - 7u_{i-4}^n}{240dx^3} \end{aligned} \right\}, \quad (2)$$

where temporal and spatial step is given by dt and dx respectively. The truncation error order of spatial discretization in Eq. 2 is . In Eq. 2, the spatial location is denoted using subscript index i and the time using superscript index n . The time integration was done using fourth order Runge-Kutta scheme. The temporal step was decided using stability analysis resulting in stability condition,

$$dt = \frac{2dx^3}{3\sqrt{3}}, \quad (3)$$

giving $dt = 3 \times 10^{-4}$ for $dx = 0.1$. The total spatial and temporal steps $n_x = 161$ and $n_t = 3000$. The numerical solution of KdV is generated using the initial condition by superimposing two solitons moving at different velocities and interacting together.

$$u(x, 0) = 0.5\operatorname{sech}^2(0.5x - 20t - 4) + 0.5\operatorname{sech}^2(0.5x - 10t + 4), \quad (4)$$

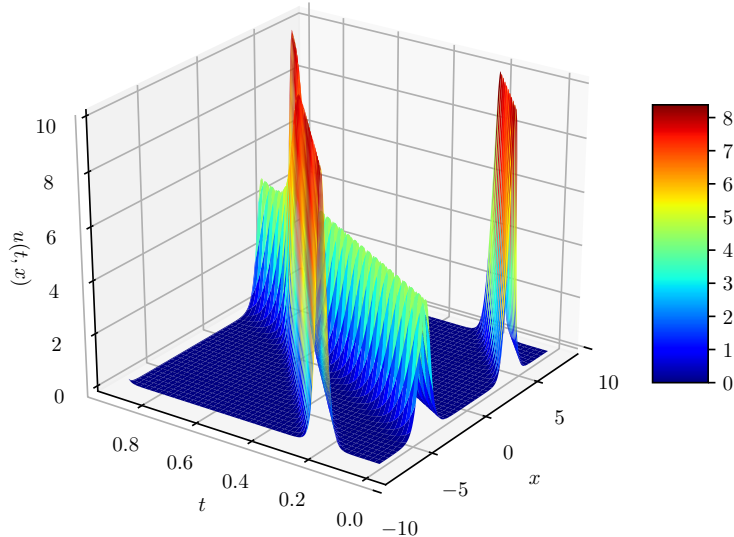


Figure 1: Numerical solution of KdV PDE

3 Data Assimilation Methodology

We use traditional (stochastic) ensemble Kalman filter (EnKF) and deterministic ensemble Kalman filter (DEnKF) approaches to predict the field from observations and perturbed initial conditions. The I.C is perturbed by 10% to generate erroneous trajectory along with adding

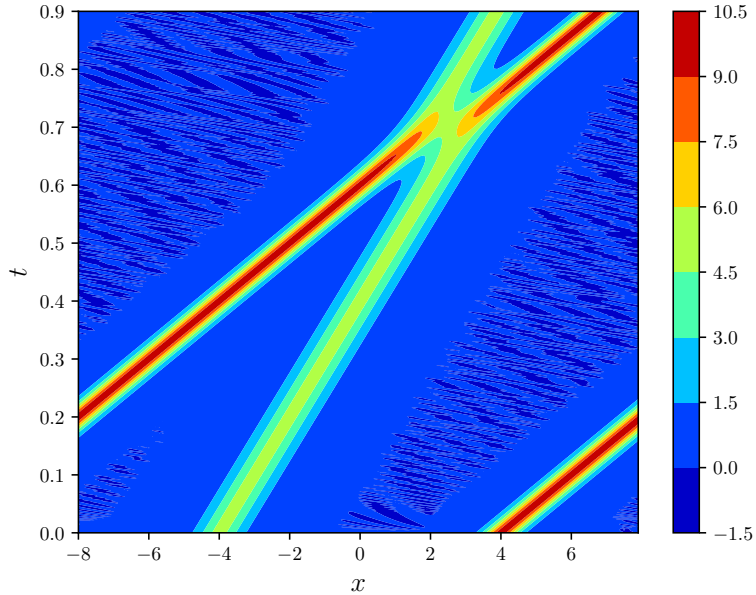


Figure 2: Contour plot of KdV numerical solution.

white Gaussian noise of varied variance (σ). The perturbed I.C is given as,

$$u(x, 0) = 1.1(0.5 \operatorname{sech}^2(0.5x - 20t - 4) + 0.5 \operatorname{sech}^2(0.5x - 10t + 4)) + \mathcal{N}(\mu, \sigma^2), \quad (5)$$

where μ is mean and σ is variance. The EnKF and DEnKF sequential algorithms are explained in detail in [2] and [4] and to that end, this report does not include the fine details of these numerical procedures. The following sections deal with performance of EnKF and DEnKF algorithms with respect to number of ensembles(n_e), observations (n_o) and noise levels controlled by variance (σ). The following discussion deals with the observations made from the Section 4 and 5.

1. Higher the number of ensembles, the better is the performance of both EnKF and DEnKF algorithms. For present KdV case, n_e of 50 is sufficient to predict the trajectory by assimilating observations. For $n_e = 10$, there is a observable lag in prediction of waves and their interactions.
2. We increased the noise by changing the variance σ . It is observed that at $\sigma = 1$ both EnKF and DEnKF algorithms predicted wrong location of point at which wave interactions occur.
3. We decreased the number of observations n_o and as expected lower the n_o , poorer the predictions of both algorithms.

4. The mean squared error between the best predicted model u^* and the true model u is given by,

$$MSE = \frac{1}{N} \sum_{l=1}^N (u_{(l)}^* - u_{(l)})^2, \quad (6)$$

where u_l^* is the value predicted field (out of N samples cases) and u_l is the true or measurement field.

4 Stochastic Ensemble Kalman Filter (EnKF)

4.1 Varying numer of ensmebles (n_e)

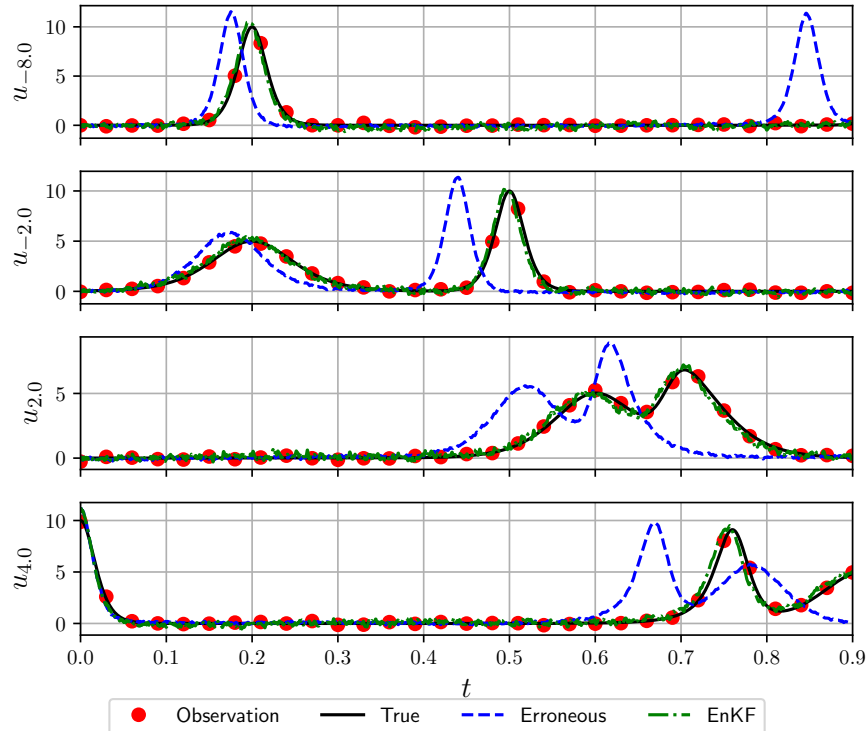


Figure 3: $n_e = 100$, $n_o = 80$ and $\sigma = 1 \times 10^{-2}$.

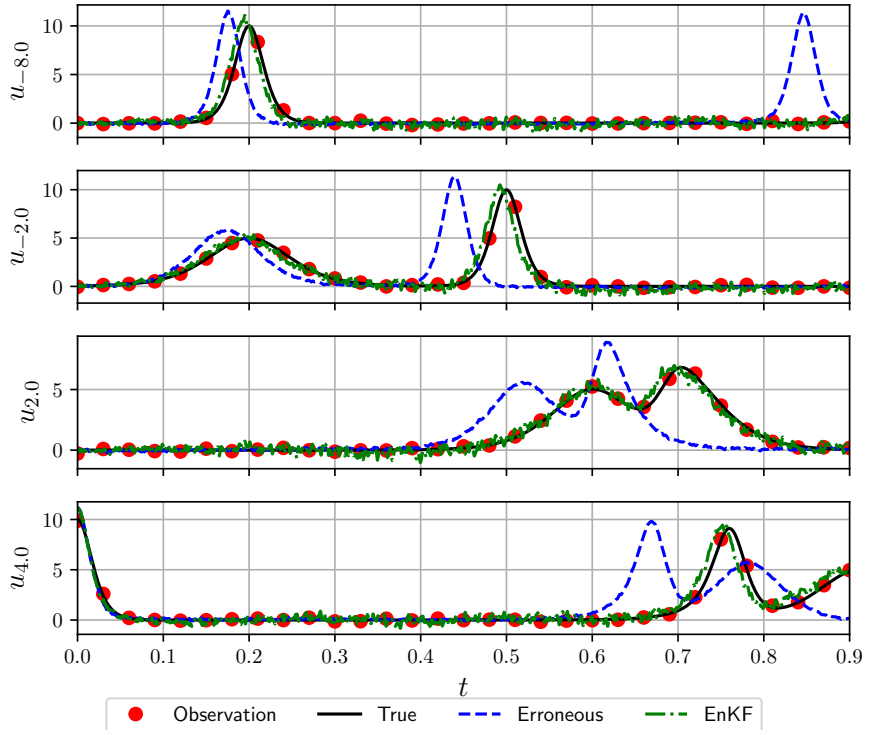


Figure 4: $n_e = 50$, $n_o = 80$ and $\sigma = 1 \times 10^{-2}$.

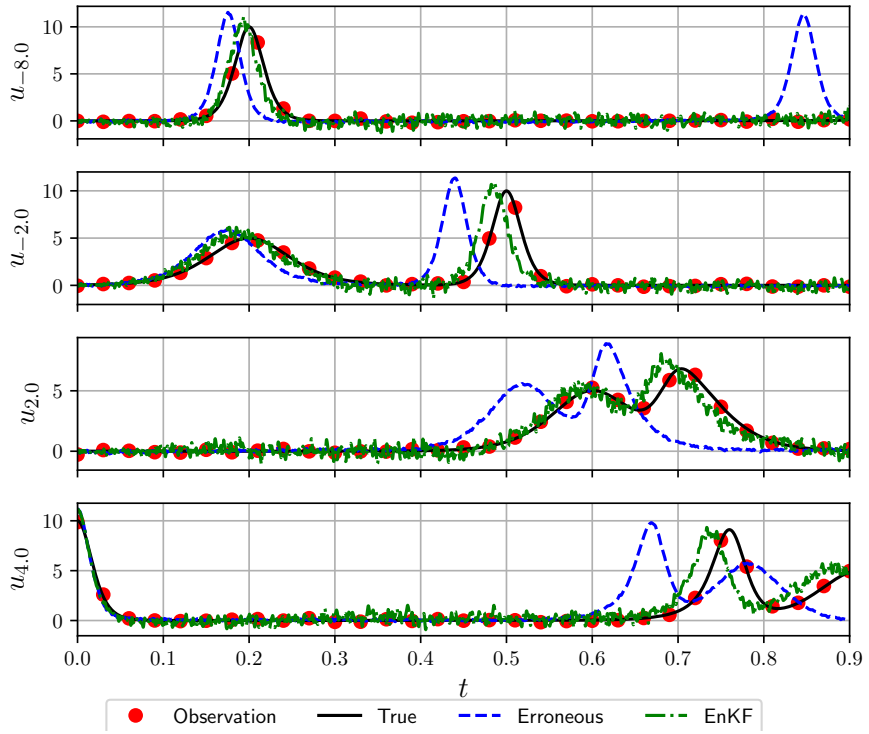


Figure 5: $n_e = 25$, $n_o = 80$ and $\sigma = 1 \times 10^{-2}$.

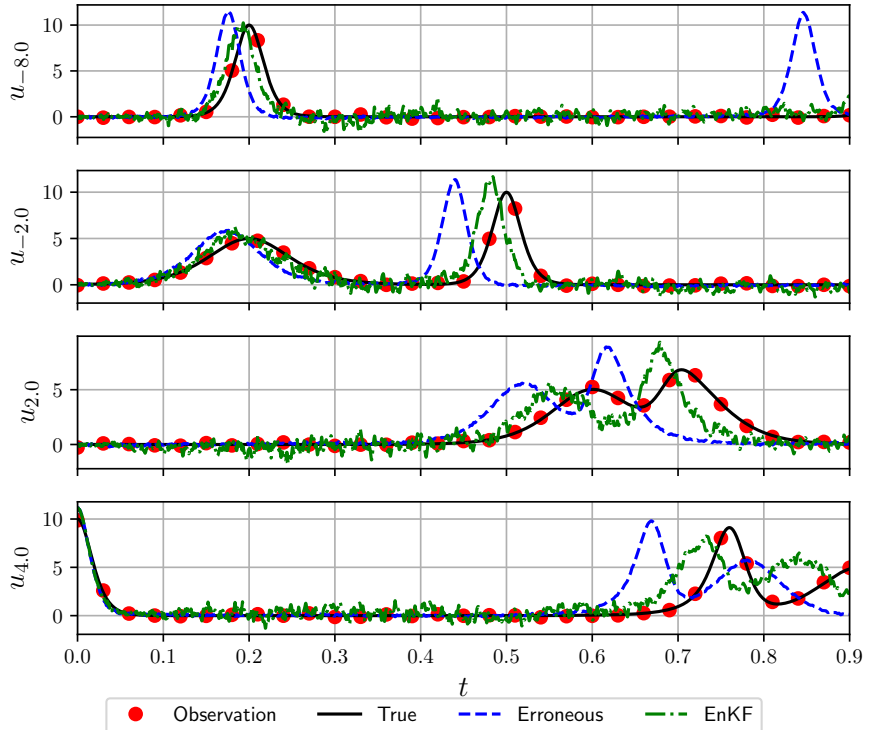


Figure 6: $n_e = 10$, $n_o = 80$ and $\sigma = 1 \times 10^{-2}$.

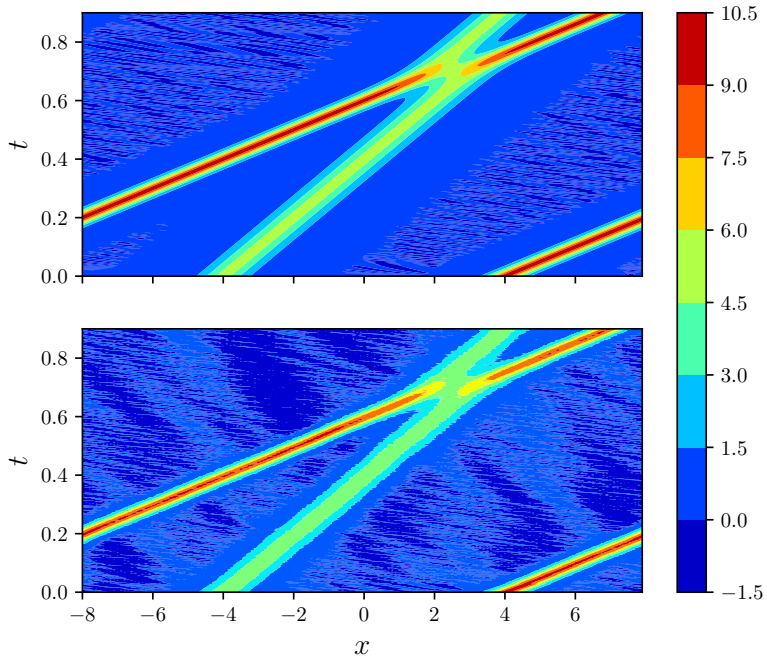


Figure 7: $n_e = 50$, $n_o = 80$ and $\sigma = 1 \times 10^{-2}$. Top plot shows true field while bottom shows EnKF predicted field.

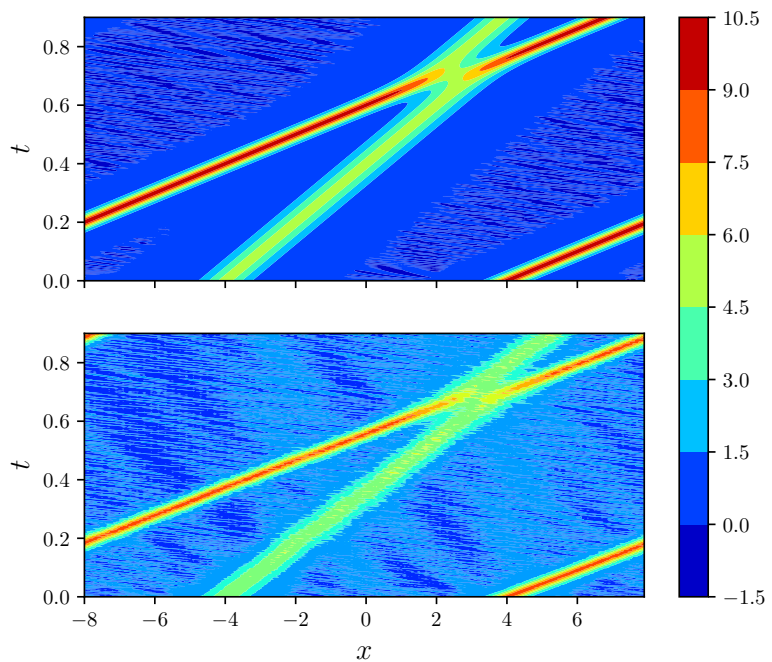


Figure 8: $n_e = 10$, $n_o = 80$ and $\sigma = 1 \times 10^{-2}$. Top plot shows true field while bottom shows EnKF predicted field.

4.2 Varying noise (σ)

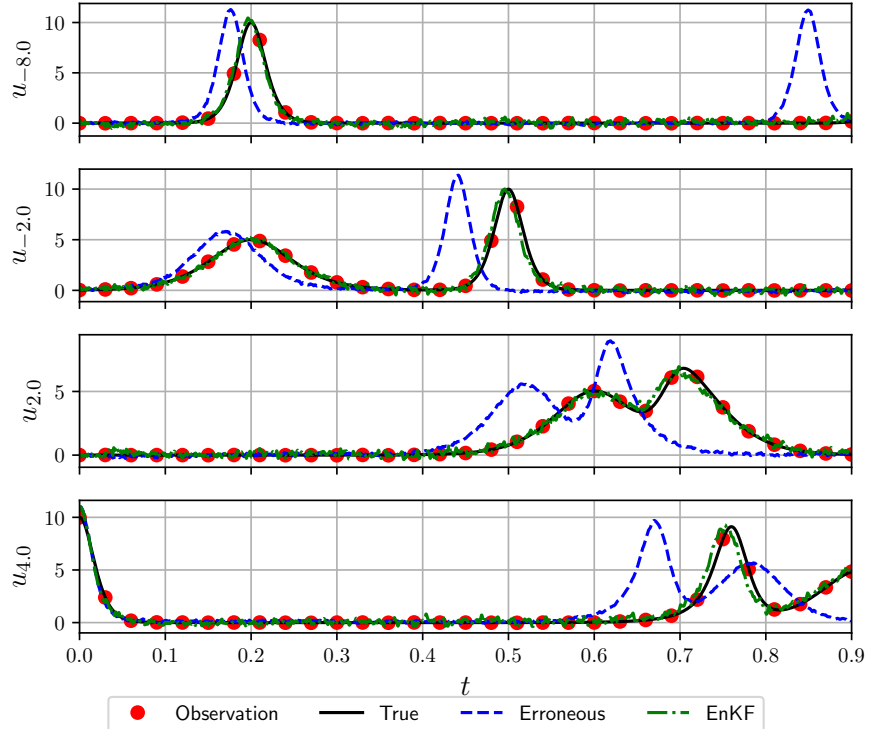


Figure 9: $n_e = 100$, $n_o = 80$ and $\sigma = 1 \times 10^{-4}$.

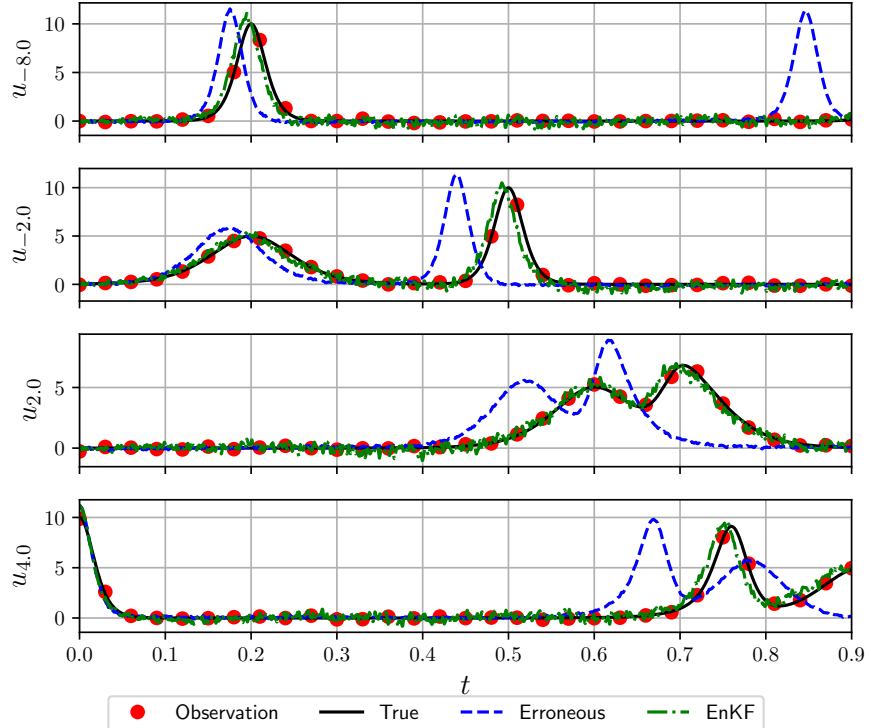


Figure 10: $n_e = 50$, $n_o = 80$ and $\sigma = 1 \times 10^{-2}$.

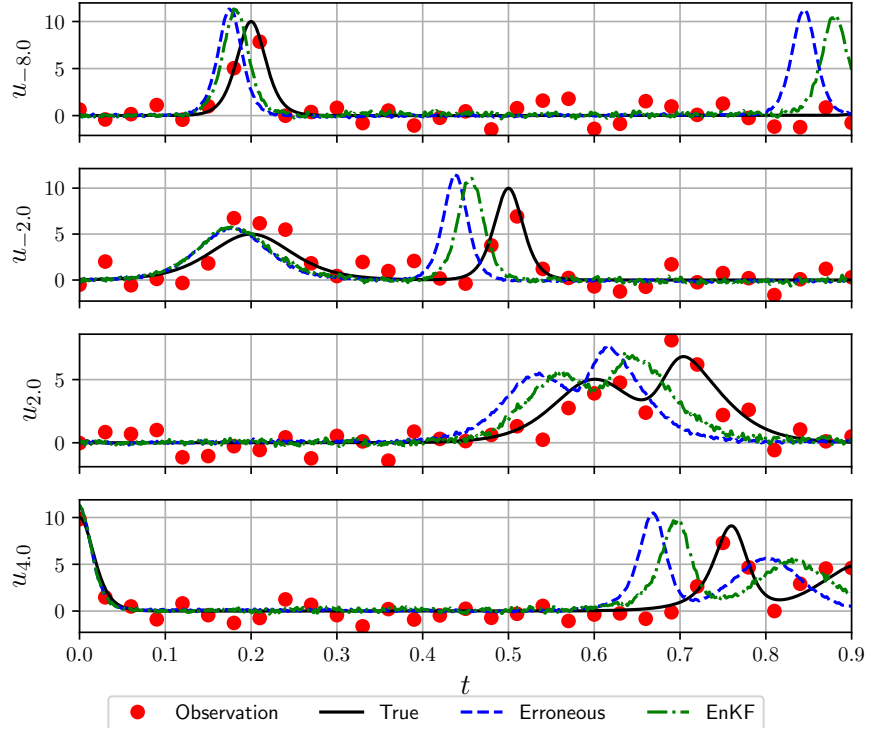


Figure 11: $n_e = 50$, $n_o = 80$ and $\sigma = 1.0$.

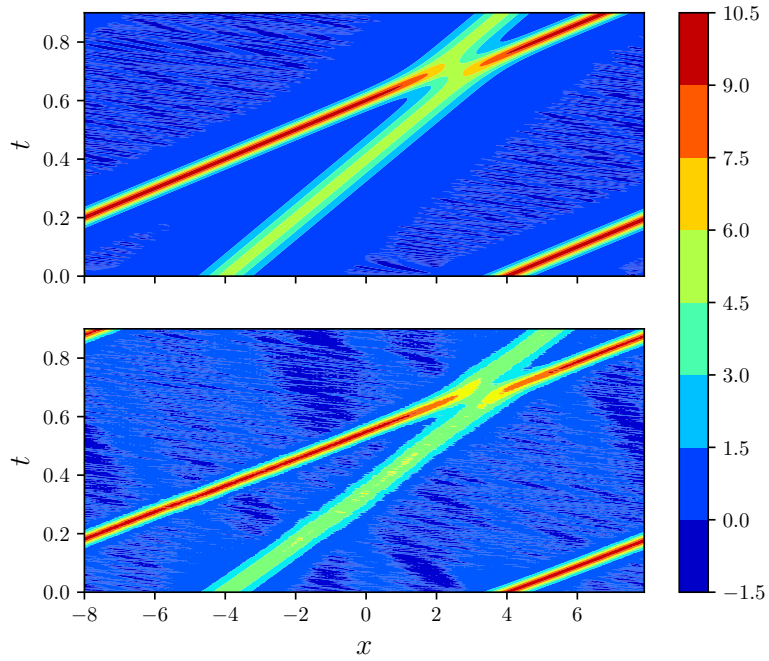


Figure 12: $n_e = 10$, $n_o = 80$ and $\sigma = 1.0$. Top plot shows true field while bottom shows EnKF predicted field.

4.3 Varying number of observations (n_o)

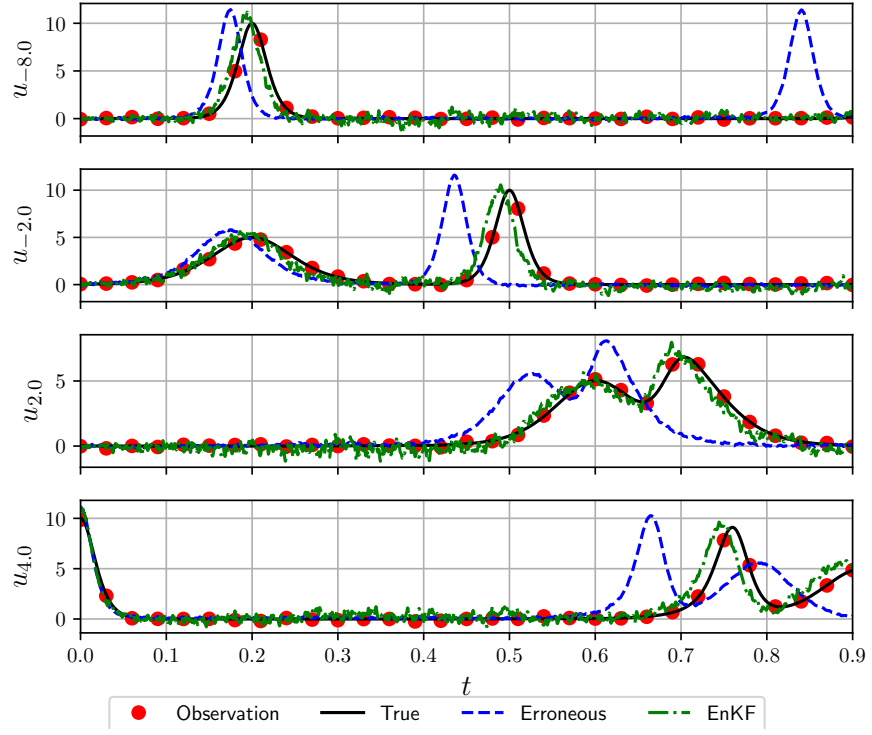


Figure 13: $n_e = 50$, $n_o = 40$ and $\sigma = 1 \times 10^{-2}$.

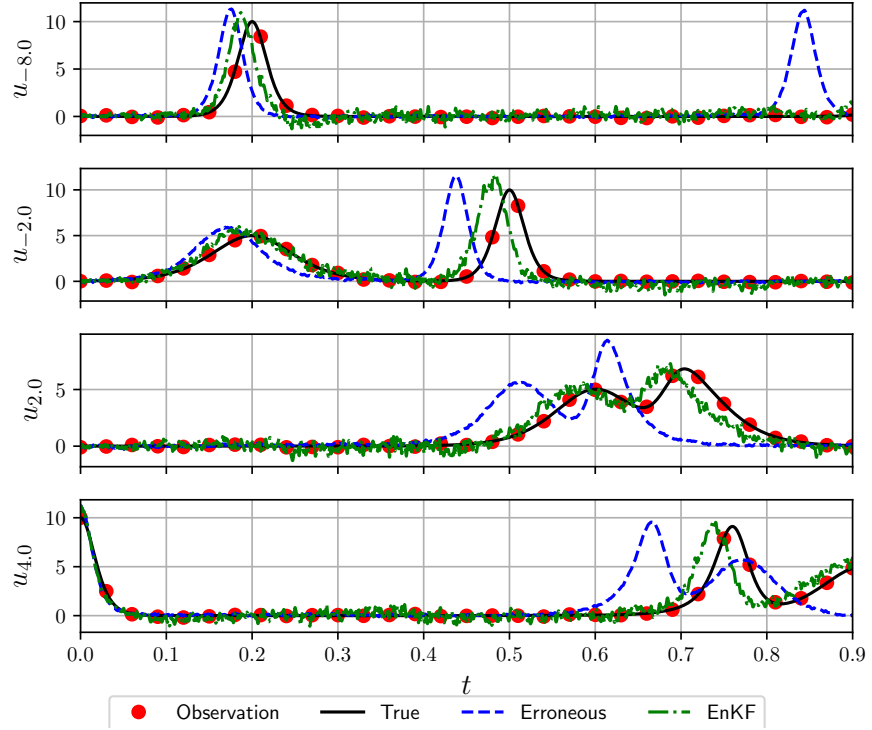


Figure 14: $n_e = 50$, $n_o = 20$ and $\sigma = 1 \times 10^{-2}$.

5 Deterministic Ensemble Kalman Filter (DEnKF)

5.1 Varying number of ensmebles (n_e)

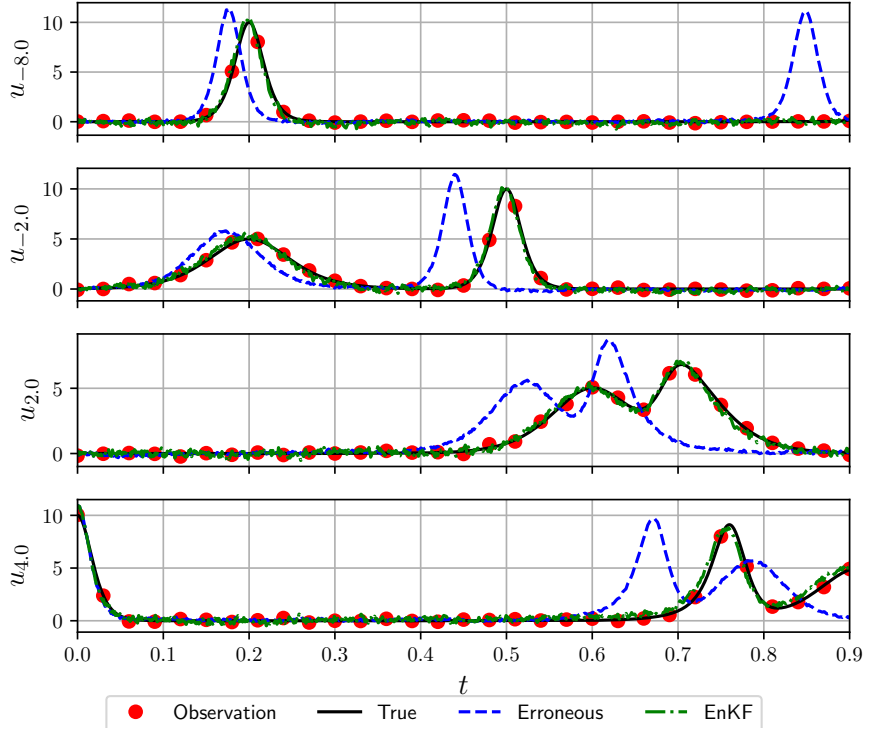


Figure 15: $n_e = 50$, $n_o = 80$ and $\sigma = 1 \times 10^{-2}$.

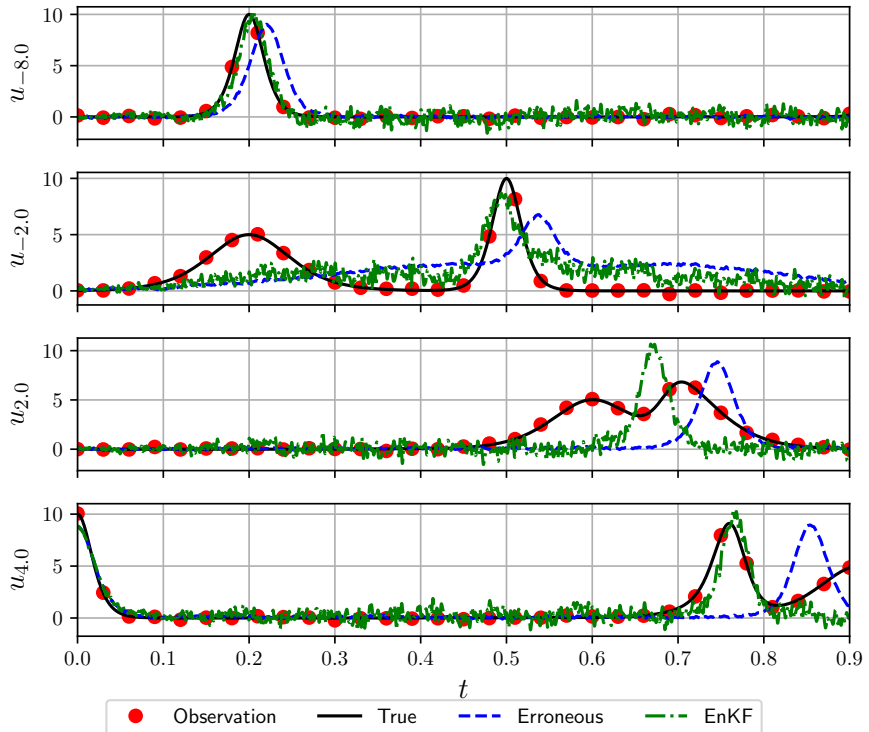


Figure 16: $n_e = 10$, $n_o = 80$ and $\sigma = 1 \times 10^{-2}$.

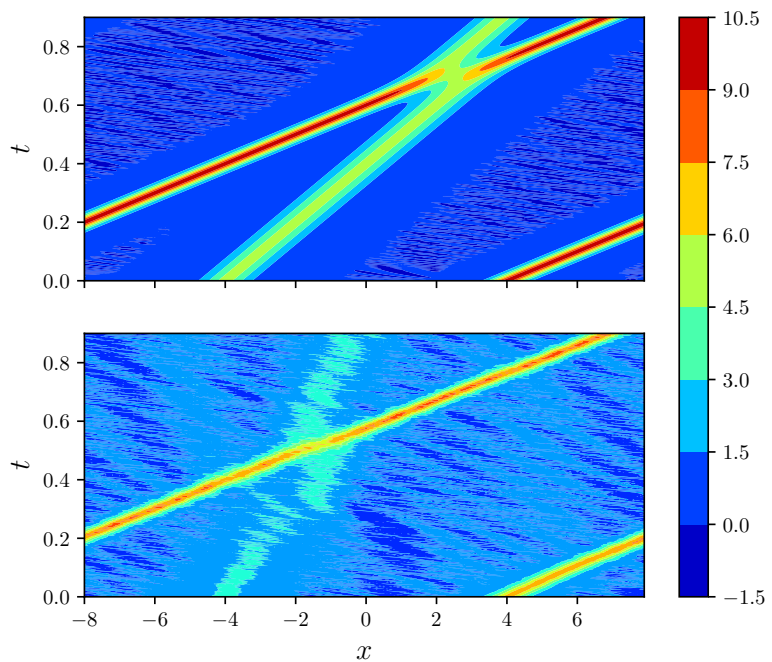


Figure 17: $n_e = 10$, $n_o = 80$ and $\sigma = 1 \times 10^{-2}$. Top plot shows true field while bottom shows EnKF predicted field.

5.2 Varying noise (σ)

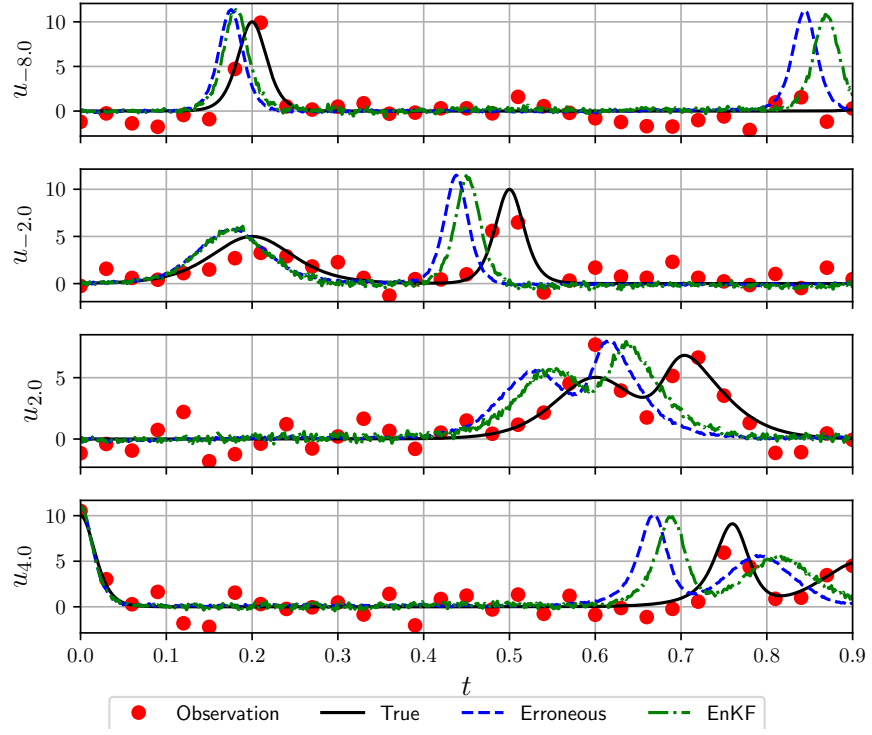


Figure 18: $n_e = 50$, $n_o = 80$ and $\sigma = 1.0$.

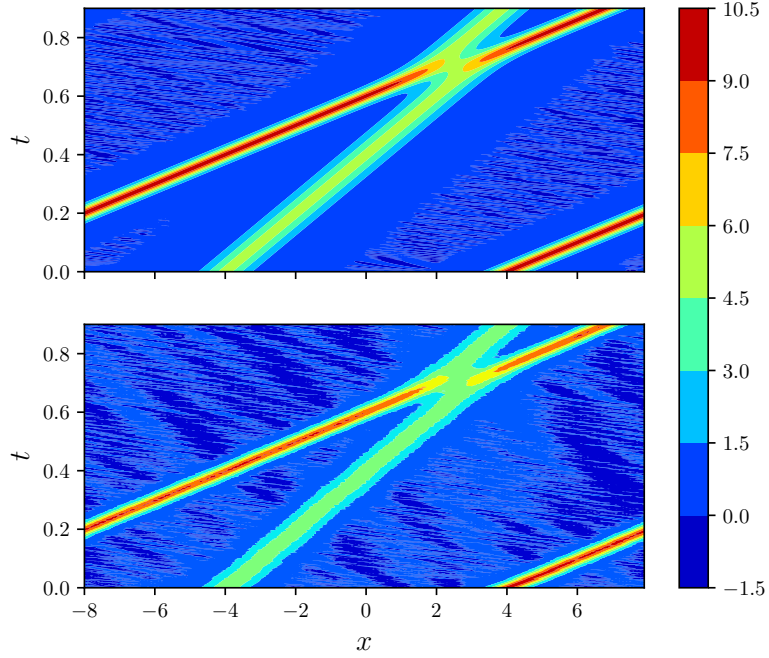


Figure 19: $n_e = 50$, $n_o = 80$ and $\sigma = 1 \times 10^{-2}$. Top plot shows true field while bottom shows DEnKF predicted field.

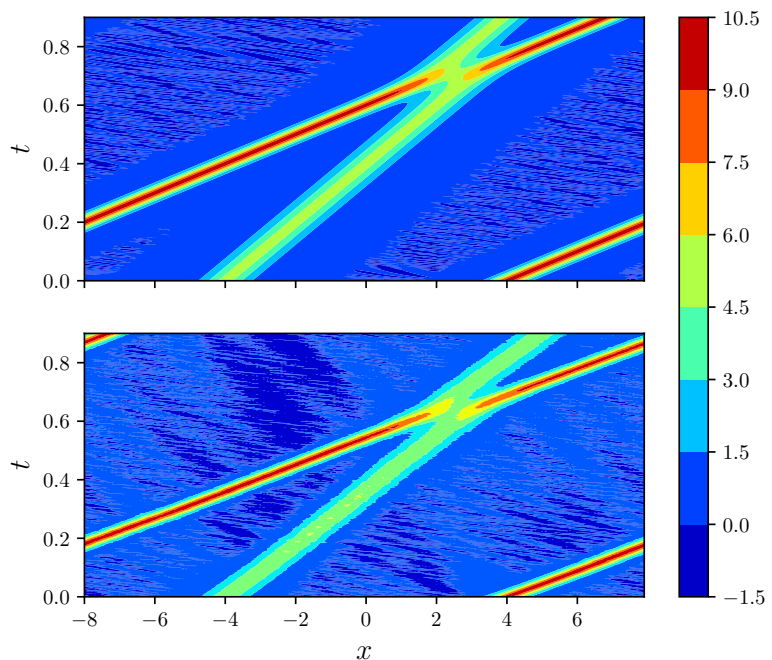


Figure 20: $n_e = 50$, $n_o = 80$ and $\sigma = 1.0$. Top plot shows true field while bottom shows DEnKF predicted field.

5.3 Varying number of observations (n_o)

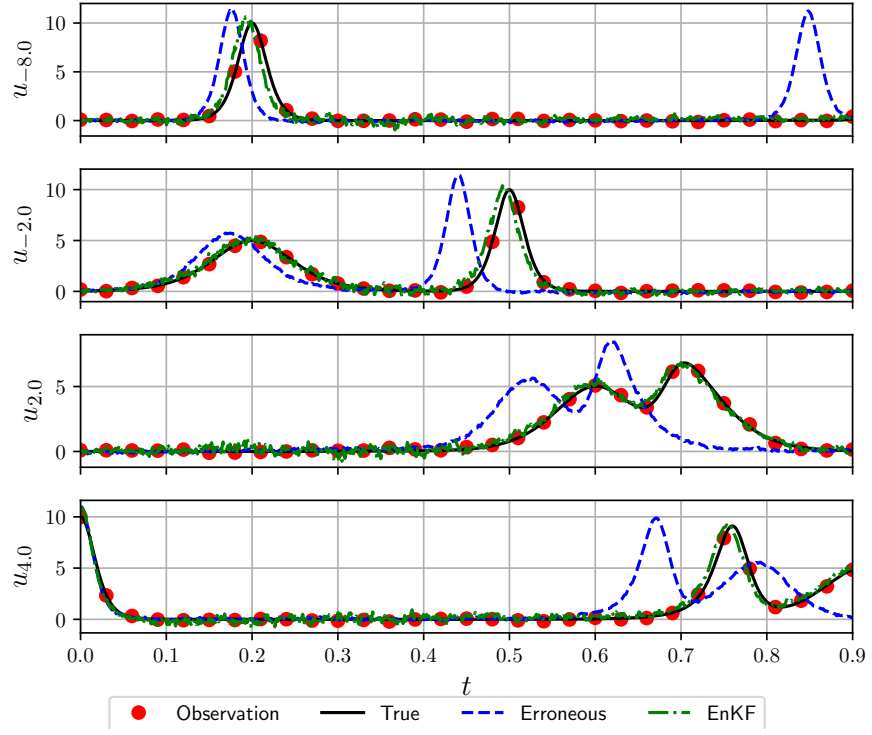


Figure 21: $n_e = 50$, $n_o = 40$ and $\sigma = 1 \times 10^{-2}$.

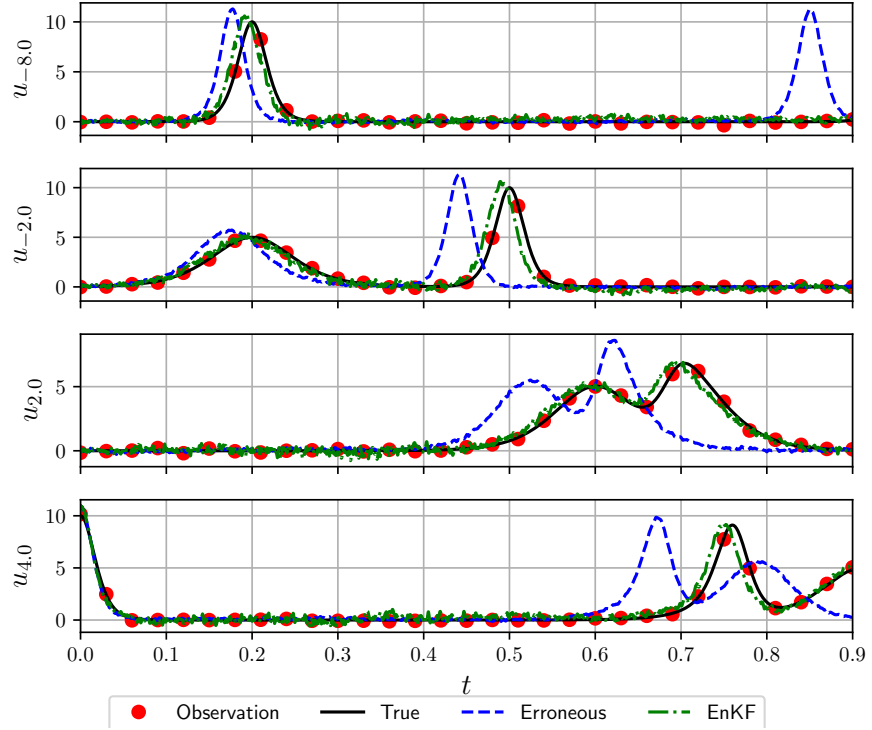


Figure 22: $n_e = 50$, $n_o = 20$ and $\sigma = 1 \times 10^{-2}$.

References

- [1] D. J. Korteweg and G. de Vries. On the change of form of long waves advancing in a rectangular canal, and on a new type of long stationary waves. *Philosophical Magazine*, 39(240):422–443, 1895.
- [2] John M Lewis, Sivaramakrishnan Lakshmivarahan, and Sudarshan Dhall. *Dynamic data assimilation: a least squares approach*, volume 13. Cambridge University Press, 2006.
- [3] T Ozis and S Ozer. A simple similarity-transformation-iterative scheme applied to Korteweg–de Vries equation. *Applied Mathematics and Computation*, 173(1):19–32, 2006.
- [4] Pavel Sakov and Peter R Oke. A deterministic formulation of the ensemble kalman filter: an alternative to ensemble square root filters. *Tellus A: Dynamic Meteorology and Oceanography*, 60(2):361–371, 2008.
- [5] Luwai Wazzan. A modified tanh–coth method for solving the KdV and the KdV–Burgers’ equations. *Communications in Nonlinear Science and Numerical Simulation*, 14(2):443–450, 2009.